Available online at www.sciencedirect.com
ScienceDirect
International Journal of Heat and Mass Transfer 50 (2007) 1269–1277
International Journal of HEAT and MASS TRANSFER
www.elsevier.com/locate/ijhmt

Chaotic mixing of fluids in a planar serpentine channel

Kuo-Wei Lin [a], Jing-Tang Yang [a,b,*]

[a] Department of Power Mechanical Engineering, National Tsing Hua University, Hsinchu 30013, Taiwan
[b] Institute of Microelectromechanical Systems, National Tsing Hua University, Hsinchu 30013, Taiwan

Received 24 February 2005; received in revised form 19 September 2006
Available online 16 November 2006

Abstract

We have achieved rapid chaotic mixing of two fluids flowing in a planar serpentine convergent–divergent mini-channel, and analyzed the transient three-dimensional flow field and distribution of concentration. The degree of irregularity of trajectories is increased through experiencing a repeated configuration of turning with an amplified pressure gradient in the designed channel. The results reveal that the pattern of the alternating convergent–divergent cross sections induces corner Dean cells with much increased Dean numbers; the stretching and folding of interfaces are effectively enhanced, resulting in superior chaotic mixing of fluids. Viewed on cross sections normal to the main stream, the complicated trajectories appear to halt, swing and twist as the fluids approach the Dean cells. Along the stream, the flow trajectories become increasingly irregular. The flow trajectories of Dean cells are symmetric with respect to the central cross section; on each side of the cross section, the flow trajectories are highly unstable, spatially and temporally, around the Dean cell. In our mixing channel the Dean cells in the mixing channel are arranged across the interfaces; the interfacial area between fluids is continuously distorted and enlarged in a spiral behavior, thus effectively promoting the fluid mixing.

Keywords: Serpentine channel; Flow structure; Chaotic mixing

1. Introduction

Fluid mixing is a key issue in contemporary systems for micro-total analysis, such as a DNA sensor [1], amino-acid detector [2] and vitamin precursor reactor [3]. Because of the large resistance and small inertia of fluids in a micro system, enhancing the mixing between liquids remains a challenge. A clarification of mixing mechanisms and efficient designs of fluidic mixers are thus urgently needed.

After visualization of the folding of colored bands in water, Reynolds first described mechanisms of fluid mixing in 1893 [4]. To improve the efficiency of fluid mixing, Welander observed and defined a chaotic feature, as a simple and regular flow with chaotic trajectories of fluid [5]. Ottino et al. [4,6–11] and Aref [5,12–14] subsequently elucidated these mechanisms: Aref achieved chaotic mixing at small Reynolds numbers with appropriate blinking-vortex flow of a two-dimensional temporally periodic model; Ottino et al. performed a two-dimensional analysis on periodic mixing with cavity flow and journal-bearing flow at small Reynolds numbers [7,8]. For a simple and robust design of fluidic mixers, chaotic mixing was achieved with an alternative approach of a spatially periodic flow, such as involving serpentine channels [13–15] and partitioned pipes [16]. Through numerical simulation, Amon [17] observed vortices and described chaotic phenomena at Reynolds number 450 in a wave-like convergent–divergent channel. Accompanying the development of micro technology, various micro-fluidic mixers have been described for which the order of Reynolds number is 10 or less [14,18–20].

For an objective of satisfactory efficiency of mixing at a small Reynolds number, chaotic mixing in a serpentine channel has attracted much attention. For a fluid flowing

* Corresponding author. Tel.: +886 3574 2916; fax: +886 3572 4242.
E-mail address: jtyang@pme.nthu.edu.tw (J.-T. Yang).

0017-9310/$ - see front matter © 2006 Published by Elsevier Ltd.
doi:10.1016/j.ijheatmasstransfer.2006.09.016

in a serpentine channel, in 1927 Dean found that counter-rotating roll cells exist at turns when the Reynolds number of flow is great enough or the turn sufficiently large. This amplitude is made quantitative as the Dean number [21], defined according to the following equation:

$$Dn = Re \cdot \sqrt{\frac{d}{R}} \tag{1}$$

Here Re is the Reynolds number, d represents the hydraulic diameter, and R is the radius of the turn. Liu et al. [14] utilized a micro scale, three-dimensional serpentine channel to induce chaotic mixing in a range 6–70 of Reynolds number. Castelain et al. [15] investigated the mixing of fluids in a three-dimensional serpentine channel, generating an irregular trajectory of fluid particles with a centrifugal force and geometrical perturbation.

Mass transfer resembles heat transfer. Peerhossaini et al. [22,23] analyzed two heat exchangers of coils over a range 141–530 of Dean number; they recorded a velocity pattern by laser Doppler velocimetry, and visualized the flow field with fluorescence. Heat transfer is enhanced through chaotic trajectories. Acharya and Sen [24] demonstrated that the flow in a coil with an alternating axis leads to chaotic trajectories of particles, thus enhancing thermal transfer. To induce secondary flow for fluid mixing, we chose a planar serpentine channel; our design resembles the alternating-axis concept of Acharya and Sen, but we incorporate alternating convergent–divergent cross sections in the channel.

2. Physical model

The designed fluidic mixer has a planar serpentine channel with alternating convergent–divergent cross sections, Fig. 1. The depth of this channel is 2.00 mm and its width is 2.00 mm at a narrow cross section or 4.00 mm at a wide cross section. Into an initially empty channel co-flow a red species and a blue species with flow velocity 80.0 mm/s after full development individually in the entrance channels. The Reynolds number, $\rho Vd/\mu$, is 160, with density $\rho = 1000\ \mathrm{kg/m^3}$, velocity $V = 80.0$ mm/s, characteristic length $d = 2.00$ mm, and viscosity $\mu = 1.00 \times 10^{-3}\ \mathrm{kg/m\,s}$. As expected, Dean cells are induced at Dean number 226. The working fluids are regarded as incompressible Newtonian liquids. An interfacial force between fluids is ignored. The Schmidt number, $\mu/\rho D$, is 500 and the Peclet number, Vd/D, is 80000; here D denotes diffusivity.

The continuity equation is

$$\frac{\partial \rho}{\partial t} + \nabla \cdot \vec{u} = 0 \tag{2}$$

The momentum equation is

$$\frac{\partial \vec{u}}{\partial t} + \vec{u} \cdot \nabla \vec{u} = -\frac{1}{\rho}\nabla p + \frac{\mu}{\rho}\nabla^2 \vec{u} \tag{3}$$

The species equation is

$$\frac{\partial C}{\partial t} + \vec{u} \cdot \nabla C = D\nabla^2 C \tag{4}$$

The pressure at the outlets is fixed at $1.0 \times 10^5\ \mathrm{N/m^2}$. At the boundary between the solid wall and the working fluid, the flow has no slip, and the local flow velocity is zero.

3. Numerical method

A time-dependent three-dimensional numerical simulation was conducted with commercial software (CFD-ACE+, CFDRC Corp., USA). The time accuracy is upgraded with a Crank–Nicolson second-order method and a blender factor 0.6. A SIMPLEC (semi-implicit method for pressure-linked equations consistent) method is adopted to solve the governing equations. All spatial discretizations are performed according to a first-order upwind scheme. The solution is considered to attain convergence when the relative difference of adjacent variables in consecutive iterations is less than 1.00×10^{-4}. Tests of mesh refinement were examined for the entrance channel with cells numbering 37440, 65472, 120988, 326400, 585648 and 1023178; the results show that the relative error of velocity of cells of number from 65472 to 1023178 is 2.89×10^{-2}. A structured hexagonal cell of size $6.09 \times 10^{-13}\ \mathrm{m^3}$ was thus chosen.

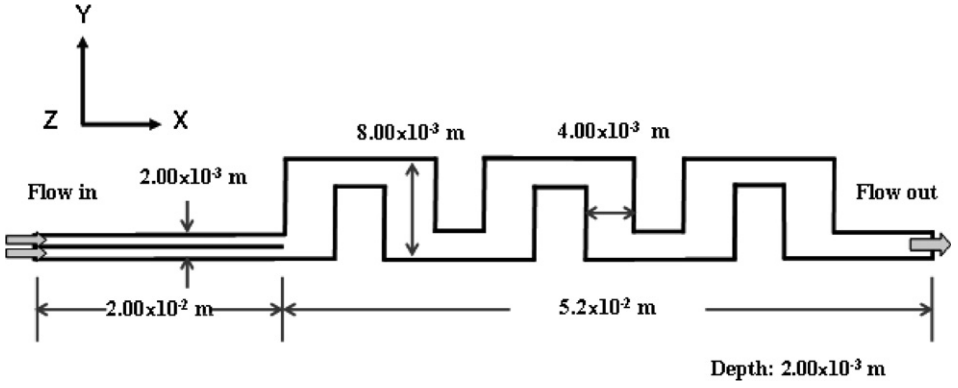

Fig. 1. Schematic diagram of the mixing channel.

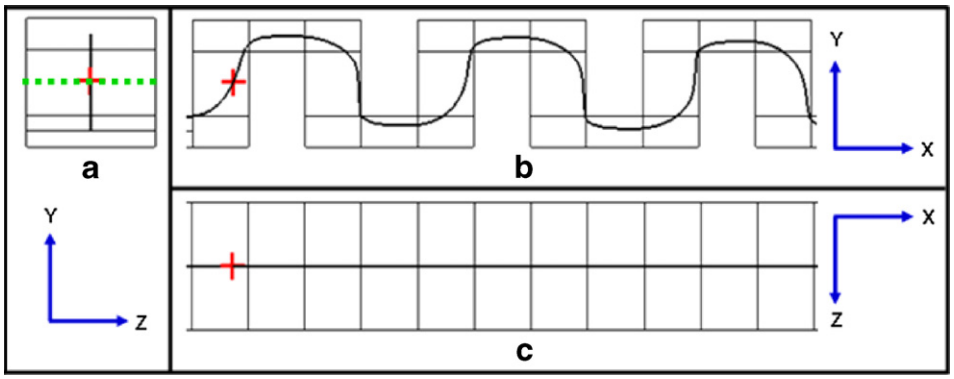

Fig. 2. Distribution of regular trajectories.

4. Results and discussion

Fluids are expected to mix via an enlargement of the interface between the fluids. Our approach is to create chaotic trajectories with flow in a planar serpentine convergent–divergent channel at an appropriate Dean number; which determines the degree of induced secondary flow. For a sufficiently large Reynolds number or curvature of turn, an adverse pressure gradient occurs, and circulating flows called Dean cells are induced. We suppose that Dean cells considerably enlarge the interface of fluids near the corners so that fluids become effectively mixed. In this case the Dean number is 226, at which creation of Dean cells is possible. To verify our hypothesis, we analyze the distributions of trajectory, fluid and flow velocity.

4.1. Trajectory distributions modes

At an early stage, no vortex forms at the corners; subsequently, vortices form, develop and become stabilized at the corners. After the flow is stabilized, the trajectory distributions are complicated and have varied degrees of regularity. The trajectory is regular when it is far from a Dean cell. As shown in Fig. 2b, these trajectories are smooth, and exhibit little disturbance in the z-direction, Fig. 2a and c. In Figs. 2a, 3a and 4a, the green dashed lines[1] designate the initial interface between the influx fluids.

As the trajectory approaches a Dean cell, the degree of distortion increases, especially in the z-direction, as in Fig. 3c. The profile of this trajectory exhibits a cyclic motion as viewed from the x-direction. As the trajectory approaches nearer a Dean cell, it shows chaotic behavior with the contour of the trajectory not returning through the repeated configuration of the channel, Fig. 4. We suggest that trajectories within the Dean cells might assist in stretching the interface between the fluids. Fluids are expected to mix effectively via the Dean cells.

To clarify the roles of various flow structures on mixing, flow is decomposed into the stages in the main stream and the corner flow, as shown in Figs. 5 and 6, respectively. The trajectories in the main stream are more regular than in the corner flow in the right and top views. These trajectories neither flow in the transverse direction nor penetrate into the corners. Trajectories of corner flow form vortices and agitate the fluid effectively. The top view of the fluid trajectories shows that the scales of vortices are smaller near the top and bottom boundaries than those in the central cross sections.

To show the intrinsic instability of fluid trajectories at the central cross section, we plot a set of individual trajectories at the middle cross section in the z-direction, Fig. 7; the corresponding trajectory of an individual fluid element is traced as shown in Fig. 8. Although the fluidic mixer has a planar design, the flow has complicated three-dimensional paths of motion. Almost all fluid trajectories demonstrate that the fluid generally flows from the central cross section in various ways. Along trajectory (a), fluid flows initially in the longitudinal direction, but flows transversely into the top corner on the left side downstream. Along trajectory (b), fluid flows initially in the longitudinal direction, and also diverts transversely to the right side; the direction of the transverse motion is unstable. For those trajectories not near vortices, the trajectories are stable and invariably flow longitudinally, as shown by lines (c, d, e) in Fig. 8. For trajectories near or passing through a vortex, the routes are unstable. Flow might be initially longitudinal but diverts into a conjugate vortex downstream, as indicated by lines (a, b, i). Otherwise, flow might initially occur within a conjugate vortex, and shift toward the longitudinal direction downstream. Adjacent vortices along the longitudinal direction might be connected and interact with each other via the same trajectory, as shown by lines (f, g, h).

The temporal variations of fluid trajectories for a fixed point near a divergent turn at the middle cross section are shown in Fig. 9. The fluid initially flows along the longitudinal direction, such as line (a). As a vortex develops, the trajectory continues to alter its direction and experiences a period of instability, before it becomes stable after 4.2 μs.

[1] For interpretation of the references to color in Figs. 2–4, the reader is referred to the web version of this article.

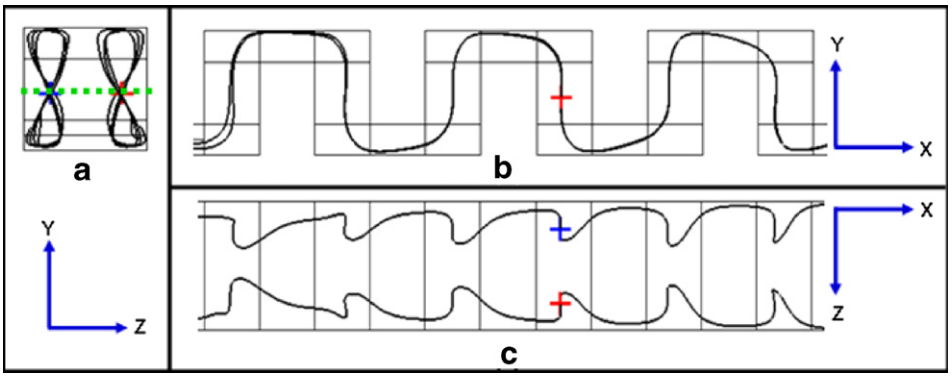

Fig. 3. Distribution of swing trajectories.

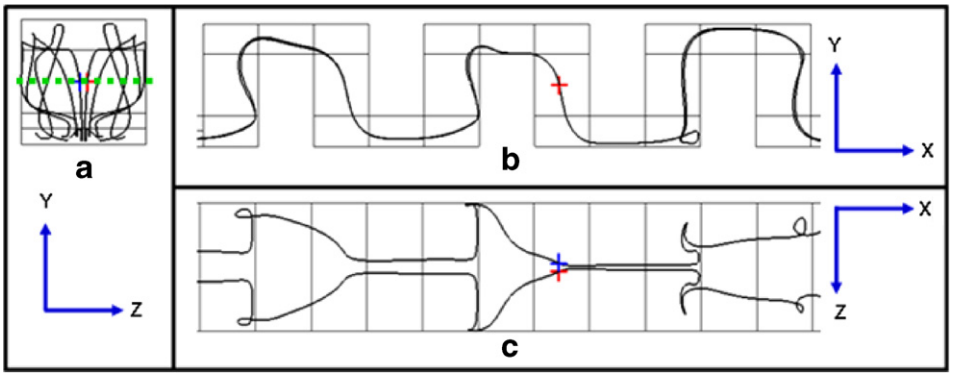

Fig. 4. Distribution of twist trajectories.

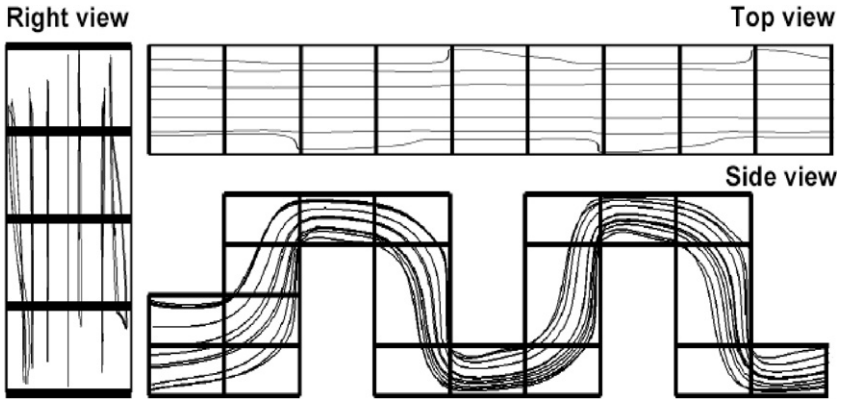

Fig. 5. Three views of the fluid trajectories of central flow.

The vortex of the divergent turn and another vortex following the convergent turn eventually become connected with the same trajectory, as indicated by line (i). Although the trajectory seems unstable at the central cross section spatially and temporally, the flow across this interface is nearly zero. Usually, these unstable trajectories do not complicate the velocity and mass fraction results, and exert only a slight effect on fluid mixing across the central plane. However, in our mixing channel the flow direction of the Dean cells is arranged across the interfaces; the interfacial area between the fluids is continuously distorted and enlarged in a spiral behavior, so effectively promoting the fluid mixing.

4.2. Swirling intensity and fluid distribution

We define the swirling intensity as the square of flow velocity projected on the analyzed cross section ($V^2 + W^2$). To understand the turning effect of the channel, we analyzed the swirling intensity and the mass fraction at 12 cross sections of the channel, which are orthogonal to

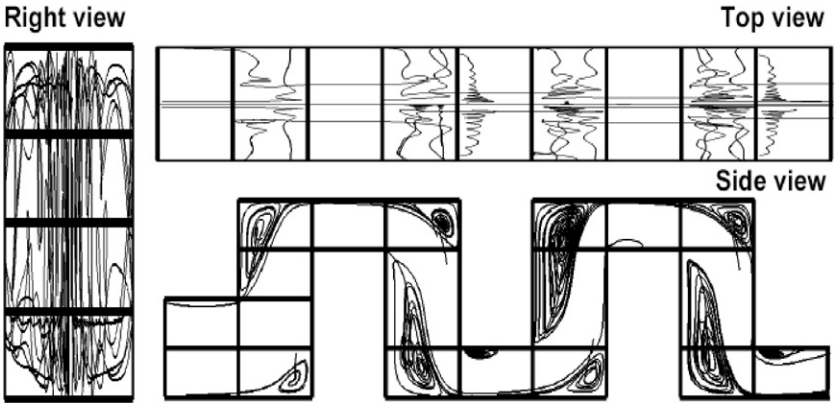

Fig. 6. Three views of the fluid trajectories of corner flow.

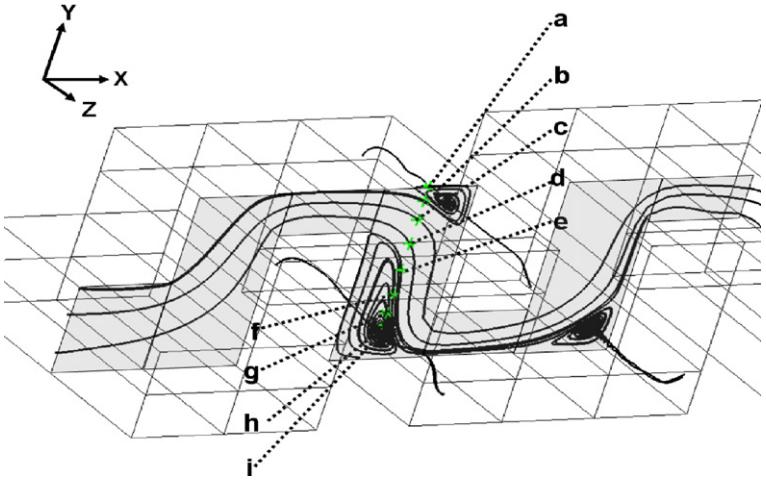

Fig. 7. Chaotic fluid trajectories in the middle cross section and the z-direction.

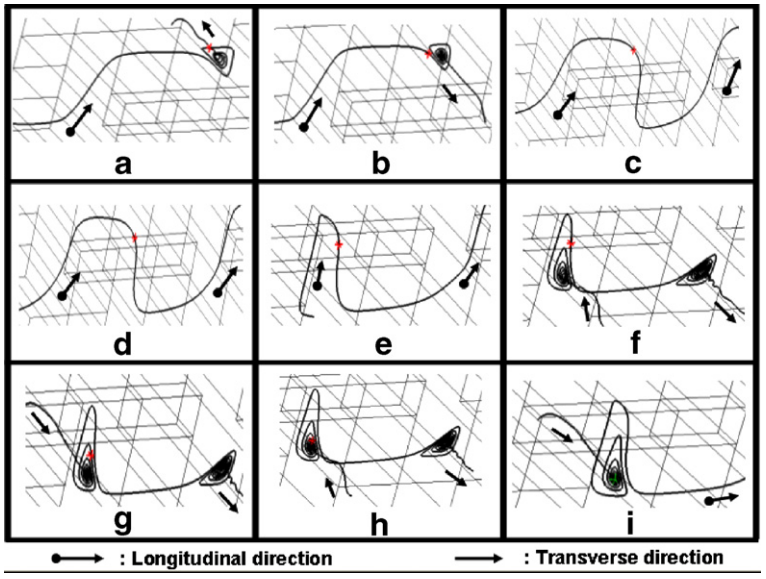

Fig. 8. Longitudinal and transverse paths of motion of the fluid trajectories at the middle cross section and the z-direction.

the x-direction as shown in Fig. 10. These cross sections occur just before and beyond a turn; in this work each turn is accompanied by an abruptly convergent or divergent cross section.

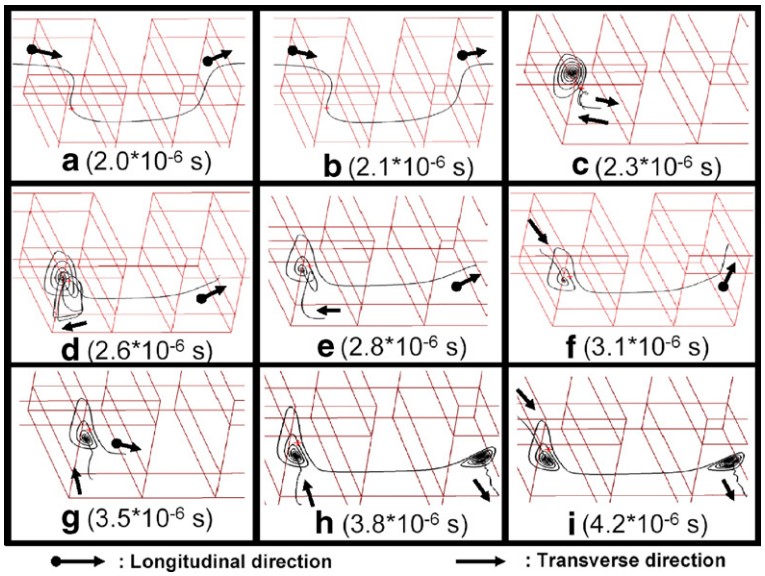

Fig. 9. Temporal variations of fluid trajectories at the middle cross section in the z-direction.

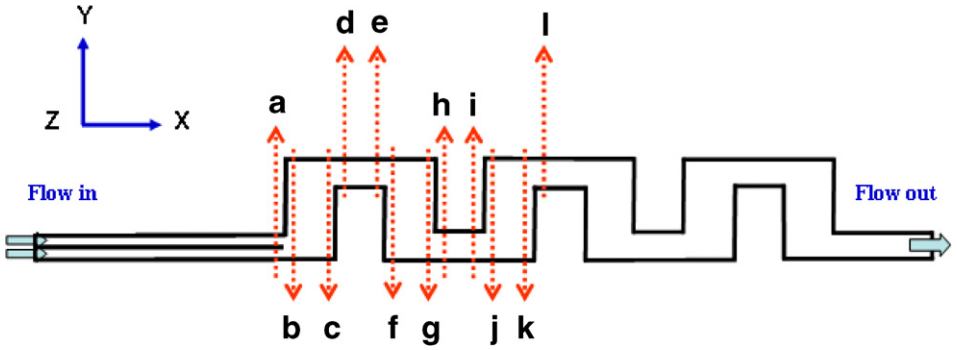

Fig. 10. Analyzed cross sections of fluid distribution and the swirling flow pattern of the channel.

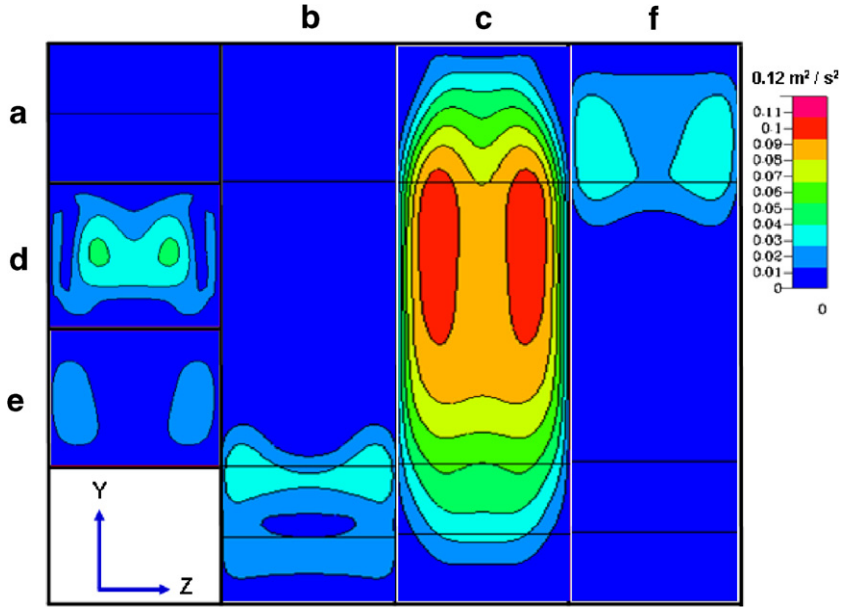

Fig. 11. Swirling intensity at the first six analyzed cross sections of the channel.

The swirling intensities on the analyzed cross sections are shown in Fig. 11. Two working fluids are fully developed before entering the serpentine channel with no swirling, Fig. 11a. As the injected stream encounters a divergent turn, it is tracked to follow the turning direction, Fig. 11b. The flow exhibits a Y-shaped pattern as the fluids flow through an upward turn. The flow near the wall is retarded by a viscous force whereas the flow near the central cross section is dominated by an inertial force. The maximum flow upward is thus between the wall and the central cross section. As the fluid flows into the suddenly convergent cross section, a pair of strongly swirling flows is formed, Fig. 11c. After a convergent turn, the swirling intensity of flow weakens immediately in a narrow cross section, Fig 11d. According to the viscous effect, the swirling intensity continuously decays, Fig. 11e. At the next divergent turn, the swirling intensity increases slightly, Fig. 11f. At the next six cross sections, the swirling intensity is repeated with flow through a repeated configuration of channel, Fig. 12. Because the Reynolds number is as small as 160, the flow disturbance is not amplified on passing through a repeated configuration of channel. Overall, the major

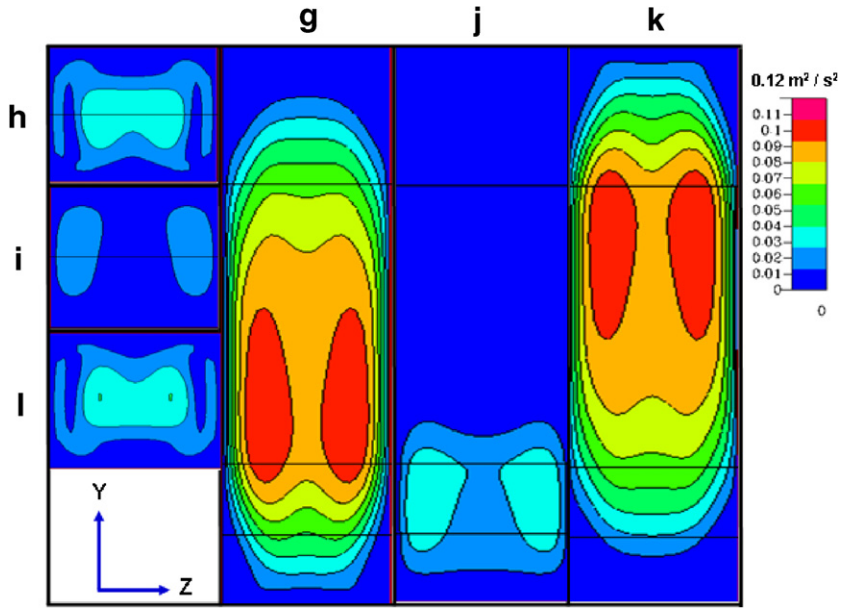

Fig. 12. Swirling intensity at the next six analyzed cross sections of the channel.

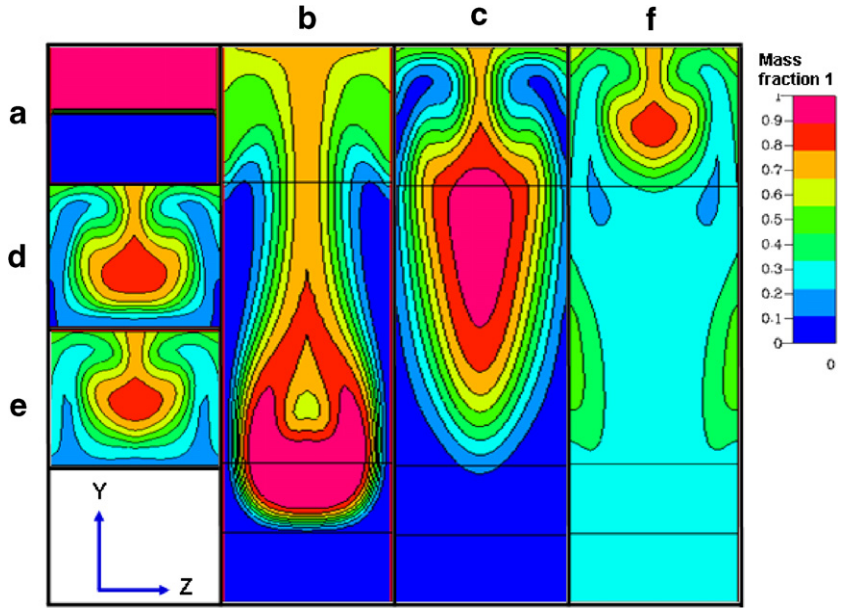

Fig. 13. Fluid distribution at the first six analyzed cross sections of the channel.

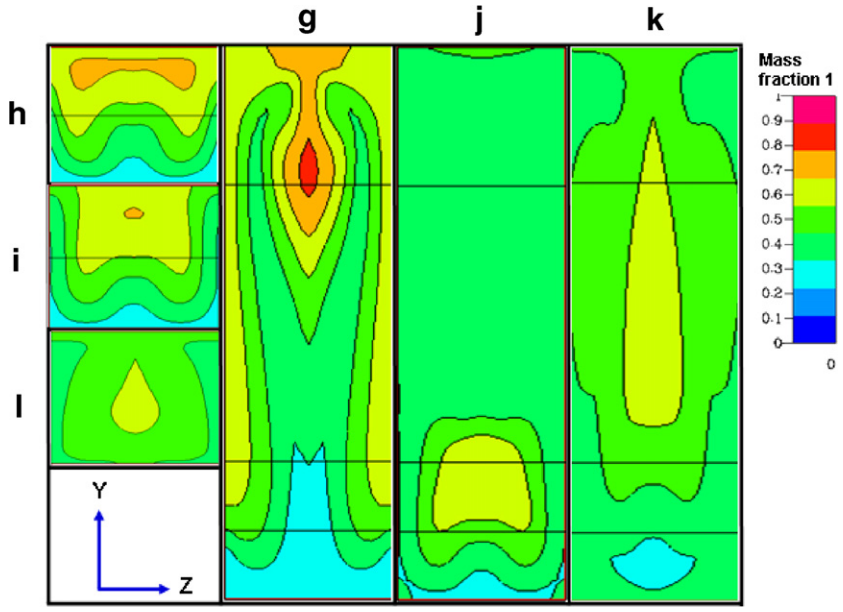

Fig. 14. Fluid distribution at the next six analyzed cross sections of the channel.

swirling intensity occurs behind a convergent turn; we suppose that the interface of fluids experiences a large distortion there, so that fluids mix effectively in this region.

Fluid is transferred in the direction of the concentration gradient (diffusion) and bulk flow (advection). Fluid distribution at 12 analyzed cross sections are depicted in Fig. 13. After the two working fluids are fully developed individually in the entrance channels, they begin to mix in the serpentine channel, Fig. 13a. Experiencing an upward diverging turn, the swirling flow makes the lower fluid envelop the upper fluid, Fig. 13b. The increased swirling flow before a convergent turn makes the lower fluid envelop the upper fluid in advance, Fig. 13c. The pattern of fluid distribution at cross section (e) is similar to that at cross section (d), because there is little or no swirling flow along the narrow channel. At the next divergent turn, the fluid experiences a downward motion; the swirling flow again distorts the interface of fluids, Fig. 13f. In summary, the interface between the fluids is greatly distorted and enlarged after a series of divergent and convergent turns. At the next analyzed six cross sections, Fig. 14, the contour of fluid distribution becomes blurred relative to Fig. 13. Fluids are mixed effectively on experiencing alternating divergent and convergent turns. The flow is not perturbed at a small flow velocity in a regular configuration of the channel. For the analyzed cross section, the non-zero velocity there makes the interface of fluids continue to fluctuate. Because the interface between the fluids is located at the Dean cell, the interfacial area is distorted and enlarged in a spiral manner. The fluid distribution varies continuously at the next Dean cell until the mixed fluid becomes uniform. Compared with the flow normal to the analyzed cross section, the large flow velocity in the cross section determines the degree of interface distortion. Fluids are mixed chaotically via regular flow and irregular trajectories in the fluids.

5. Conclusion

In this work we achieve rapid chaotic mixing of two fluids flowing in a planar serpentine convergent–divergent mini-channel. The transient three-dimensional flow field and fluid distribution at Reynolds number 160, Schmidt number 500, Péclet number 80000, and Dean number 226 are numerically analyzed. The degree of irregularity of swinging and twisted flow trajectories is increased through experiencing a repeated configuration of turning with an amplified pressure gradient in the designed channel. The results reveal that the pattern of the alternating convergent–divergent cross sections induces corner Dean cells with much increased Dean numbers; the stretching and folding of interfaces is hence effectively enhanced, and a superior chaotic mixing of fluids is consequently achieved.

At Schmidt number 500, molecular diffusion is much slower than momentum diffusion. Molecular diffusion does not affect the flow pattern, which is dependent solely on the Reynolds number. The laminar flow at Reynolds number 160 inhibits the flow disturbances and results in a similar velocity configuration in repetitive sectors. At Péclet number 80000, the degree of mixing is determined by the residence period and the interfacial area of fluids.

In the development stage after the entrance, a pair of Dean cells is induced, grows, and finally turns stabilized around the corners, and which considerably enlarge the interface of fluids near the corners. Viewed on the cross sections normal to the main stream, the trajectories are complicated and appear to halt, swing and twist as the fluids

approach the Dean cells. Along the stream, the flow trajectories become increasingly irregular. The entire flow trajectories of Dean cells are symmetric with respect to the central cross section. On each side of the cross section, the flow trajectories are highly unstable, spatially and temporally, around the Dean cells. In our mixing channel the flow direction of the Dean cells is arranged across the interfaces; the interfacial area between the fluids is continuously distorted and enlarged in a spiral behavior, so effectively promoting the fluid mixing.

Acknowledgement

National Science Council of the Republic of China provided financial support under contracts NSC 92-2212-E-007-044 and NSC 92-2212-E-007-045.

References

[1] M.A. Burns, B.N. Johnson, S.N. Brahmasandra, K. Handique, J.R. Webster, M. Krishnan, T.S. Man, P.M. Jones, D. Heldsinger, D. Mastrangelo, C.H. Sammarco, D.T. Burke, An integrated nanoliter DNA analysis device, Science 282 (1998) 484–487.
[2] D.J. Harrison, K. Fluri, N. Chiem, T. Tang, Z. Fan, Micromachine chemical and biochemical analysis and reaction systems on glass substrates, Sensor Actuator B 33 (1996) 105–109.
[3] H. Löwe, W. Ehrfeld, State of the art in microreaction technology: concepts, manufacturing and applications, Electrochim. Acta 44 (1999) 3679–3689.
[4] J.M. Ottino, S.C. Jana, V.S. Chakravarthy, From Reynolds stretching and folding to mixing studies using horseshoe maps, Phys. Fluids 6 (1994) 685–699.
[5] H. Aref, The development of chaotic advection, Phys. Fluids 14 (2002) 1315–1325.
[6] J.M. Ottino, The Kinematics of Mixing: Stretching, Chaos and Transport, Cambridge University Press, Cambridge, 1989, pp. 1–3.
[7] J.M. Ottino, C.W. Leong, P.D. Swanson, Morphological structures produced by mixing in chaotic flows, Nature 333 (1988) 419–425.
[8] W.L.D.V. Chien, H. Rising, J.M. Ottino, Laminar mixing and chaotic mixing in several cavity flows, J. Fluid Mech. 170 (1986) 355–377.
[9] J.M. Ottino, F.J. Muzzio, M. Tjahjadi, J.G. Franjione, S.C. Jana, H.A. Kusch, Chaos, symmetry, and self-similarity: exploiting order and disorder in mixing processes, Science 257 (1992) 754–760.
[10] D.V. Khakhar, H. Rising, J.M. Ottino, Analysis of chaotic mixing in two model systems, J. Fluid Mech. 172 (1986) 419–451.
[11] G.O. Fountain, D.V. Khakhar, I. Memic, J.M. Ottino, Chaotic mixing in a bounded three-dimensional flow, J. Fluid Mech. 417 (2000) 265–301.
[12] H. Aref, Stirring by chaotic advection, J. Fluid Mech. 143 (1984) 1–21.
[13] S.W. Jones, O.M. Thomas, H. Aref, Chaotic advection by laminar flow in a twisted pipe, J. Fluid Mech. 209 (1989) 335–357.
[14] R.H. Liu, M.A. Stremler, K.V. Sharp, M.G. Olsen, J.G. Santiago, R.J. Adrian, H. Aref, D.J. Beebe, Passive mixing in a three-dimensional serpentine microchannel, J. Microelectromech. Syst. 9 (2000) 190–197.
[15] C. Castelain, A. Mokrani, Y.L. Guer, H. Peerhossaini, Experimental study of chaotic advection regime in a twisted duct flow, Eur. J. Mech. B 76 (2001) 205–232.
[16] F.H. Ling, Chaotic mixing in a spatially periodic continuous mixer, Phys. Fluids 5 (1993) 2147–2160.
[17] C.H. Amon, Lagrangian chaos, Eulerian chaos, and mixing enhancement in converging–diverging channel flows, Phys. Fluids 8 (1996) 1192–1206.
[18] R. Miyake, T.S.J. Lammerink, M. Elwenspoek, J.H.J. Fluitman, Micro mixer with fast diffusion, in: Proceedings of the Micro Electro Mechanical Systems, MEMS'93, Fort Lauderdale, Florida, USA, 1993, pp. 248–253.
[19] N. Schwesinger, T. Frank, H. Wurmus, A modular microfluid system with an integrated micromixer, J. Micromech. Microeng. 6 (1996) 99–102.
[20] A.D. Stroock, S.K.W. Dertinger, A. Ajdari, I. Mezić, H.A. Stone, G.M. Whitesides, Chaotic mixer for microchannels, Science 295 (2002) 647–651.
[21] W.R. Dean, Note on the motion of fluid in a curved pipe, Philos. Mag. 4 (1927) 208–223.
[22] Y.L. Guer, H. Peerhossaini, Order breaking in Dean flow, Phys. Fluids A 3 (1991) 1029–1032.
[23] H. Peerhossaini, C. Castelain, Y. Le Guer, Heat exchanger design based on chaotic advection, Exp. Therm. Fluid Sci. 7 (1993) 333–344.
[24] N. Acharya, M. Sen, Heat transfer enhancement in coiled tubes by chaotic mixing, Int. J. Heat Mass Transfer 35 (1992) 2475–2489.